*Journal of Marine Research, 72,* 219–242, 2014

# Available energy of the world ocean

**by Peter R. Bannon[1,2] and Raymond G. Najjar[1]**

ABSTRACT

The available energy of the ocean is the excess of the sum of the ocean's internal and gravitational energies with respect to its equilibrium state, which is in thermodynamic equilibrium and has the same total entropy as the ocean. The equilibrium state for the world ocean is rigorously determined to be an isothermal ocean with a temperature of 3.66°C and a horizontally uniform absolute salinity that increases monotonically from 27.30 g $kg^{-1}$ at the surface to 47.39 g $kg^{-1}$ at a depth of 5.5 km. This salinity profile is consistent with a uniform relative chemical potential of 47.44 J $g^{-1}$ salt. The ocean's available energy is $220 \times 10^{21}$ J or 630 MJ $m^{-2}$. Most (72%) of the available energy is due to the internal energy difference between the ocean and its equilibrium state; the remaining 28% is due to the gravitational energy difference. The ocean's available energy is shown to be concentrated vertically in the upper half kilometer and geographically in the tropics and subtropics. This distribution is accurately represented by the temperature variance from the equilibrium temperature. The contributions of sea ice and variable sea surface height to the available energy are estimated to be small.

*Keywords.* global ocean energetics, available energy, available potential energy, ocean entropics

## 1. Introduction

The energy that drives the ocean circulation comes from the work done by the winds and the tides and from the fluxes of thermal energy and freshwater at the sea surface. Some of this energy input is stored as gravitational and internal energy that is available to be converted to kinetic energy. Quantifying this available energy is thus a central goal of physical oceanography. Several attempts to quantify this energy have been made for selected ocean regions and systems (Bray and Fofonoff 1981; Reid et al. 1981) as well as for the global ocean (Oort et al. 1989, 1994; Huang 2005). These attempts build upon the concept of Lorenz's (1955) available potential energy that measures the work done during the adiabatic rearrangement of individual fluid parcels. However, a more general definition of the available energy is afforded by the concept of availability.

A formal definition of the available energy of a thermodynamic system is provided by the availability function $\delta A$ that represents the amount of work obtainable from the system

1. Department of Meteorology, The Pennsylvania State University, University Park, PA 16802.
2. Corresponding author ***e-mail: bannon@ems.psu.edu***

relative to a "dead" reference state, one that is in thermodynamic equilibrium (motionless, hydrostatic, isothermal, and with uniform chemical potential). This work excludes the "*pdV*" work of expansion between the system and its equilibrium (Bannon 2012). Other appellations of the available energy include free energy, exergy, entropic energy, and maximum work (Landau and Lifshitz 1980; Bejan 2006; Tailleux 2013a). Bannon (2012, 2013) shows that the availability function satisfies the relation

$$\delta A\,(T_r) = \delta TE\,(T_r) - T_r \delta S\,(T_r)\,, \tag{1}$$

where $T_r$ is the temperature of the reference state, the total energy $TE$ is the sum of the internal and gravitational energies ($TE = IE{+}GE$), and $S$ is the total entropy. The availability is defined for the given system of interest and, for that system, is only a function of the reference temperature $T_r$. The availability is the integral over the mass $m$ of the system $\delta A = \int \delta a\, dm$ of the specific availability defined by

$$\delta a = \delta h - T_r \delta s - \alpha \delta p - \mu_r \delta \chi, \tag{2}$$

where $h$, $s$, and $\alpha$ are the specific enthalpy, entropy, and volume, respectively, $T$ is the absolute temperature, and $p$ is the pressure. The relative chemical potential is $\mu = \mu_{salt} - \mu_{water}$, and the concentration $\chi$ is given by the absolute salinity $\chi = S_A$. A reference value is denoted by a subscript $r$. State variables of the system are functions of position $\mathbf{x} = (x, y, z)$ and time $t$, but the reference enthalpy, entropy, pressure, and salinity are only functions of height $z$ as required for a motionless reference state. The chemical potential of the reference state $\mu_r$ is a constant, as required by thermodynamic equilibrium. The symbol $\delta$ defines a finite departure of the system from the reference state (Fig. 1). For example, the specific internal energy departure is $\delta u = u(\mathbf{x}, t) - u_r(z)$. The total mass of the system and that of the reference state are the same but the volumes of the two may differ (Fig. 1). Furthermore, the reference ocean has a sea surface that coincides with a geopotential surface, whereas the ocean's surface departs from a geopotential surface as a result of winds, tides, and air–sea fluxes of energy and freshwater. Then the difference in, say, the total entropy is $\delta S = S - S_r = \int (\rho s - \rho_r s_r) dV_m$, where the respective densities vanish in the appropriate regions of the total material volume $V_m$.

The maximum available energy $AE$ of a system is given by the minimum of the availability $\delta A$ at the reference temperature $T_r = T_0$ and salinity $S_{Ar} = S_{A0}(z)$ such that there is no total entropy difference between the system and the reference state. That reference state is defined to be the *equilibrium* state of the system. Then because $\delta S(T_0) = 0$, we have from (1)

$$AE = \delta A\,(T_0) = \delta TE\,(T_0)\,. \tag{3}$$

It is noted that the equilibrium temperature $T_0$, the equilibrium salinity profile $S_{A0}(z)$, and the available energy are thermodynamic state variables of the geophysical system. (Here

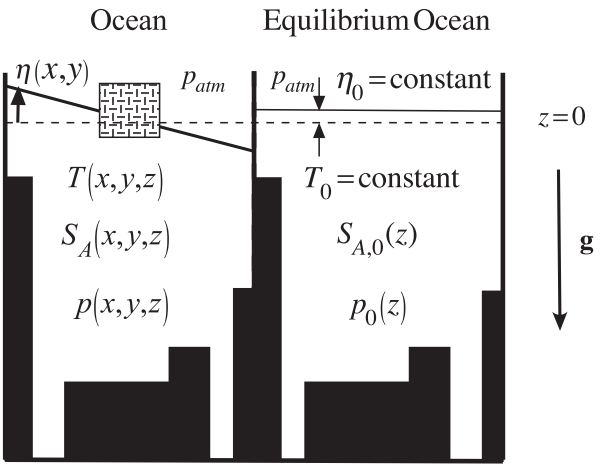


Figure 1. Schematic diagram of the ocean and its equilibrium ocean. The equilibrium ocean is hydrostatic and isothermal and has the same total mass and salt content as the ocean. The equilibrium ocean's vertical salinity and pressure gradients offset to produce an equilibrium state with uniform chemical potential. Both the ocean and its equilibrium are subject to the same uniform atmospheric pressure $p_{atm}$. The sea surface of the equilibrium ocean corresponds to a geopotential surface. The equilibrium ocean is a dynamically and convectively "dead" state.

and elsewhere a subscript zero is used to denote a quantity evaluated in the equilibrium state of the system.) It should be noted that this equilibrium state differs from that obtained if the ocean were to be isolated and slowly equilibrated adiabatically. In this case diffusive processes would have increased the total entropy of the system.

A quantity related to available energy is the available potential energy *APE* (Lorenz 1955; Tailleux 2013a) that represents the difference in the total energy of the system and its adiabatically adjusted reference state. The crucial distinction is that, in the APE theory, individual parcels are rearranged isentropically while in availability theory the system as a whole is reconfigured isentropically. The *APE* is the sum of an available gravitational energy *AGE* and an available internal energy *AIE*: $APE = AGE + AIE$, where

$$AGE = \int g\,(z - z_a)dm \quad \text{and} \quad AIE = \int (u - u_a)dm. \tag{4}$$

Here the subscript $a$ denotes the adiabatically adjusted state (i.e., individual parcels are rearranged isentropically) and $u$ is the specific internal energy. Huang (2005) presents a review of oceanic *APE* theory. We note several of its salient results. Firstly, the dominant term is the available gravitational energy *AGE* with the smaller available internal energy being negative. The positive *AGE* implies that the center of mass has been lowered during the adjustment to the reference state. The negative *AIE* is attributed (Bray and Fofonoff 1981) to the nonlinear thermodynamics of seawater as follows. On average during the adjustment

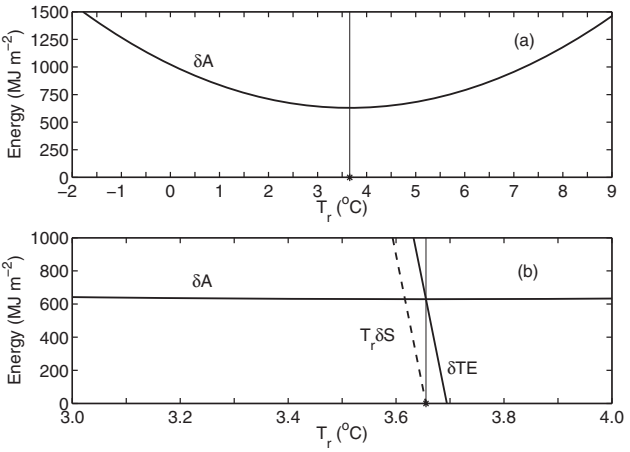


Figure 2. Availability function $\delta A$ as a function of the reference temperature $T_r$. Panel (b) is a magnified version of panel (a). The vertical line in each panel denotes the equilibrium temperature $T_0 = 3.66°\text{C}$, denoting the function's minimum. In panel (b) the tilted solid and dashed lines denote the departure in total energy $\delta TE$ and entropy term $T_r \delta S$. At the equilibrium temperature, $\delta S = 0$ and the available energy is $AE = \delta TE(T_0) = 630\ \text{MJ m}^{-2}$.

process, the denser sinking water parcels are colder than the rising warmer parcels. The rising parcels are adiabatically cooled more than the sinking parcels are adiabatically warmed. This asymmetry leads to a negative *AIE*. Secondly, the *AIE* and *AGE* may be combined using the hydrostatic assumption into an available enthalpic energy $AHE = \int (h - h_a) dm$ plus several boundary terms that require the determination of the change in volume of the system and change in bottom pressure distribution. Thirdly, and most importantly, the determination of the adiabatic reference state remains an unsolved problem. [Huang (2005, 145) notes that his numerical algorithm obtains the gravitational minimum state and not necessarily the state with minimum total energy.] Progress on this issue is ongoing (Tailleux 2013b). An approximate formulation of the *AGE* has been applied to the world's ocean (e.g., Oort et al. 1989) as available gravitational potential energy (*AGPE*) in the form

$$AGPE = \frac{g}{2} \int \frac{(\rho - \bar{\rho})^2}{\left(-d\bar{\rho}^{\theta}/dz\right)} dV, \tag{5}$$

where $\rho^{\theta}$ is the potential density and an overbar denotes a horizontal average. Typically the variance in the density field in the numerator decreases less rapidly with depth than the stability term in the denominator of the integrand (e.g., Oort et al. 1989). Thus, the resulting integrand displays an unphysical increase with depth. As a consequence, the *AGPE* approach is limited to the upper portions of the domain.

In this paper we rigorously determine the available energy of the world ocean by an exact determination of the equilibrium state. The ocean is treated as a fully compressible fluid.

Section 2 describes the world ocean data set and the analysis procedures used to evaluate the availability function $\delta A$ and determine the equilibrium state of the world ocean. The current analysis improves on that in Bannon (2013), which ignores horizontal and seasonal variability and assumes an equilibrium ocean with uniform salinity. Here the equilibrium salinity profile increases with depth such that the equilibrium relative chemical potential is uniform. This uniformity is required by the oceanic proof of the result (1). Section 3 describes the attributes of the available energy of the world ocean. Section 4 compares the present results with prior results and includes estimates of the contribution of sea ice and variable sea surface height to the available energy. Section 5 discusses how available energetics provides a framework for determining the relative roles of thermal and mechanical forcing of the ocean circulation.

## 2. World ocean and its equilibrium

### *a. Global ocean data*

The data sets employed are the seasonal- and annual-mean World Ocean Atlas 2009 (WOA09) temperature (Locarnini et al. 2010) and practical salinity (Antonov et al. 2010) fields, which reside on a $1^\circ \times 1^\circ$ latitude-longitude grid (centered on the half-degree grid points) at up to 33 standard levels in the vertical. The vertical grid is nonuniform with levels at depths of 0, 10, 20, …, 4,500, 5,000, and 5,500 m. Midpoints are defined between successive levels. When computing vertical integrals, the data at each level are taken to represent the layer between successive midpoints except for the surface and bottom layers. Level 1 data are taken to represent the layer between 0 and 5 m, and data at the deepest level at a given location represent the layer between the bottom level and the midpoint above it (Levitus 1982). The data from all marginal seas (e.g., Baltic, Black, and Red Seas) are included except those for the region of the Caspian Sea, a landlocked lake.

### *b. Data analysis*

The thermodynamic properties of the data are analyzed with the Gibbs Sea Water Oceanographic Toolbox of the Thermodynamic Equation of Seawater - 2010, TEOS-10 (McDougall and Barker 2011). In this formulation, the zero point for the entropy and enthalpy of seawater is defined as that at standard atmospheric pressure (101,325 Pa), a temperature of 0°C, and an absolute salinity of $S_A = 35.16504$ g kg$^{-1}$ (Feistel 2008). The pressure and absolute salinity fields associated with the WOA09 data (temperature and practical salinity as a function of depth) are determined iteratively assuming hydrostasy and using the TEOS-10 conversion from practical salinity to absolute salinity (which itself is a function of pressure). This procedure employs eight iterations to ensure that the pressure converges to within 0.001 dbar. The temperature data are then adjusted for values below freezing. For example, of the 1,155,406 grid points in the annual-mean data set, 1,727 points failed the test by being below freezing. These points had their temperatures increased to a hundredth of a degree above freezing. The maximum temperature increase is 0.18°C with a mean

Table 1. Regional distribution of physical properties.

| Region | Area ($10^{12}$ m$^2$) | Volume ($10^{15}$ m$^3$) | Mean depth (m) | Mass ($10^{18}$ kg) |
|---|---|---|---|---|
| Arctic | 12.18 | 19.52 | 1,602 | 20.20 |
| North Atlantic | 43.70 | 159.13 | 3,642 | 165.14 |
| South Atlantic | 33.68 | 145.34 | 4,315 | 150.90 |
| Southern Atlantic | 11.86 | 43.60 | 3,677 | 45.25 |
| Total Atlantic | 101.42 | 367.59 | 3,625 | 381.50 |
| North Pacific | 79.12 | 348.19 | 4,401 | 361.62 |
| South Pacific | 76.18 | 301.30 | 3,955 | 312.55 |
| Southern Pacific | 20.04 | 77.77 | 3,881 | 80.70 |
| Total Pacific | 175.33 | 727.25 | 4,148 | 754.87 |
| Indian | 59.21 | 238.91 | 4,035 | 247.90 |
| Southern Indian | 13.92 | 56.34 | 4,047 | 58.48 |
| Total Indian | 73.13 | 295.25 | 4,037 | 306.38 |
| World ocean | 349.89 | 1,390.10 | 3,973 | 1,442.74 |

Table 2. Regional distribution of annual-mean thermodynamic properties: mass-weighted mean salinity and temperature.

| Region | Absolute salinity (g kg$^{-1}$) | Temperature (°C) |
|---|---|---|
| Arctic | 34.93 | −0.17 |
| North Atlantic | 35.28 | 5.44 |
| South Atlantic | 34.96 | 3.76 |
| Southern Atlantic | 34.81 | 0.35 |
| Total Atlantic | 35.08 | 3.87 |
| North Pacific | 34.76 | 3.48 |
| South Pacific | 34.83 | 4.07 |
| Southern Pacific | 34.79 | 1.62 |
| Total Pacific | 34.79 | 3.53 |
| Indian | 34.94 | 4.31 |
| Southern Indian | 34.81 | 0.86 |
| Total Indian | 34.91 | 3.65 |
| World ocean | 34.89 | 3.64 |

increase of the adjusted points equal to 0.03°C. The analysis employs an acceleration due to gravity $g$ set to a latitude of 45° and includes a linear vertical depth dependence.

Tables 1 and 2 summarize the geometrical and mean physical properties of the three oceans (Atlantic, Pacific, and Indian) and related regions. Following the WOA09, the Arctic Ocean is considered to be part of the Atlantic Ocean. The Atlantic and Pacific Oceans are partitioned into regions north (northern latitudes) and south (southern latitudes north of 50°S) of the equator. The three oceans are further divided at longitudes 20°, 147°, and 292° into a southern region (latitudes south of 50°S) that together sum to form the Southern

Ocean surrounding Antarctica. Comparison of the data in Table 1 with that in Oort et al. (1989) indicates that the surface areas are similar but that the WOA09 ocean is about 233 m deeper and has a mass about 5.6% larger. The state variables (Table 2) are consistent with other studies (e.g., Oort et al. 1989). For example, the North Atlantic is the saltiest, the North Pacific the freshest, and the Indian the warmest.

*c. The equilibrium ocean*

The equilibrium ocean with temperature $T_0$ has the same entropy as the real ocean [$\delta S(T_0) = 0$] such that its available energy is given by (3). In equilibrium, there can be no diffusive fluxes of heat or salt (e.g., Fofonoff 1962). Proper treatment of diffusion must consider the effects of pressure as well as temperature and concentration gradients (Landau and Lifshitz 1987). For simplicity we follow Fofonoff (1962) and treat the dissolved salts in seawater as a single component, ignoring individual ions. Then the condition of no diffusive fluxes requires the temperature and relative chemical potential to be uniform with a salinity gradient that balances the barodiffusive effects of the vertical pressure gradient required by hydrostasy. One finds [Appendix B of McDougall and Barker (2011)] that the salinity gradient must satisfy

$$\frac{dS_A}{dz} = -g\beta^t / (\partial\mu/\partial S_A)\,, \tag{6}$$

where $\beta^t = (1/\rho)(\partial\rho/\partial S_A)_{T,p}$ is the coefficient of saline contraction. This salinity gradient is typically between $-3$ and $-4$ g kg$^{-1}$ km$^{-1}$ [in agreement with Fofonoff (1962)] and increases in magnitude approximately linearly with depth. This structure primarily reflects that of the saline contraction term, whose vertical dependence dominates the salinity gradient (6). The equilibrium salinity profile for a given isothermal ocean is found iteratively subject to the constraint (6) and the requirement of mass conservation. In practice, the salt conservation constraint is applied first to determine the salinity profile over 64 iterations. The thickness of the surface grid box of the equilibrium ocean is then adjusted over 16 iterations to ensure the conservation of total mass. This procedure yields the sea surface height $\eta_0$ of the equilibrium ocean (Fig. 1) and its virtually constant relative chemical potential $\mu_0$ of 47.44 J g$^{-1}$ salt with a standard deviation of $5 \times 10^{-5}$ J g$^{-1}$.

The equilibrium temperature is determined by finding the minimum of the availability function (1). The variation of the availability $\delta A = \int \rho\delta a\, dV$ with the reference temperature $T_r$ is depicted in Figure 2 for the annual-mean data set. One finds the minimum occurs at the equilibrium temperature $T_0 = 3.65535$°C with a mean salinity of 34.8945 g kg$^{-1}$. [The excessive number of significant figures for the equilibrium temperature arises from the need to satisfy the relation (3) at equilibrium such that $\delta A = \delta TE$.] This minimum occurs where the total entropy difference between the ocean and its reference ocean vanishes and, by (1), the function equals the difference in total energy between the ocean and its equilibrium. Then the available energy $AE$ is $220 \times 10^{21}$ J or 629.6 MJ m$^{-2}$. The effect of the marginal

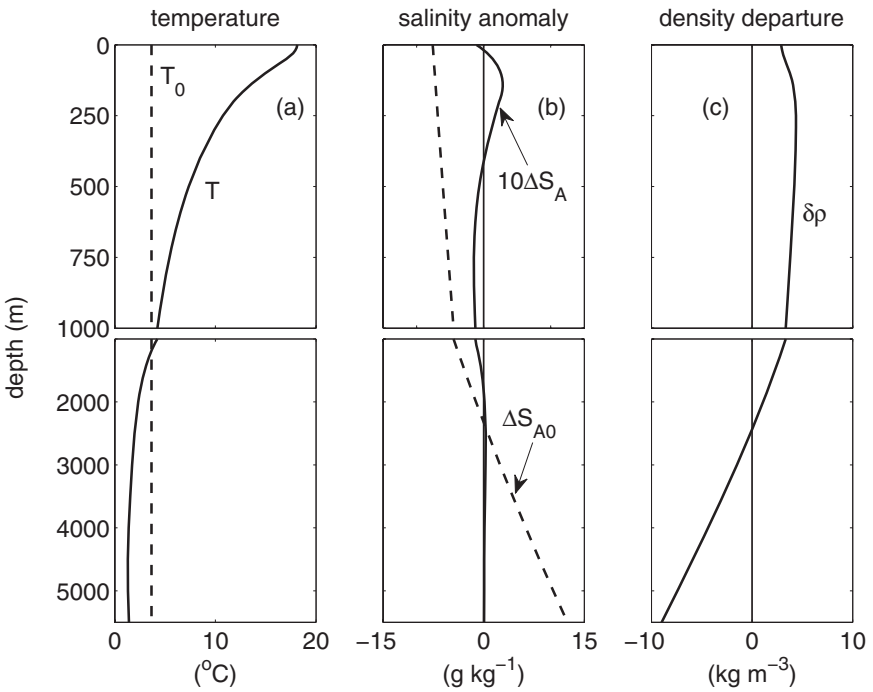


Figure 3. Vertical profiles of the horizontal mean (solid curve) and equilibrium (dashed curve) (a) temperature, (b) salinity anomaly $\Delta S_A = S_A - \bar{S}_A$ (relative to the mean value of $\bar{S}_A = 34.89$ g kg$^{-1}$), and (c) density departure $\delta\rho = \rho - \rho_0$. The ocean's horizontal mean salinity anomaly is multiplied by a factor of 10 in panel (b). The thin vertical lines represent the reference lines of zero in panels (b) and (c).

seas is assessed in a separate calculation without the Hudson Bay, the Persian Gulf, and the Mediterranean, Black, Baltic, and Red Seas. The values of the equilibrium temperature and mean salinity shift slightly lower to 3.6230°C and 34.888 g kg$^{-1}$ with a reduction in the available energy by 0.75%. All subsequent results presented here include all marginal seas (except the Caspian).

The temperature, salinity, and density of the equilibrium ocean are compared to the ocean's horizontal means in Figure 3. The ocean is warmer, on average, than its equilibrium state above a depth of 1.18 km and cooler below. The salinity of the equilibrium ocean increases monotonically from the surface value of 27.30 g kg$^{-1}$ to the deepest (5.5 km) value of 47.39 g kg$^{-1}$. (This maximum value is well below the saturation value of 360 g kg$^{-1}$ for sodium chloride.) The ocean's mean salinity profile differs significantly from the equilibrium salinity profile, with saltier waters below 2.3 km and fresher waters above. This difference indicates that the ocean's salinity profile is well stirred compared to its equilibrium. The density departure $\delta\rho = \rho - \rho_0$ indicates that the equilibrium ocean is more stably stratified than the mean ocean, with heavier fluid below a depth of 2.4 km and lighter

Table 3. Budget of the annual-mean ocean for total mass $M$, total salt *SALT*, internal energy *IE*, gravitational energy *GE*, total energy $TE = IE + GE$, and entropy $S$.

| Property | Ocean | Equilibrium |
|---|---|---|
| $M$ (Gg m$^{-2}$) | 4.1235 | 4.1235 |
| *SALT* (Mg m$^{-2}$) | 143.886 | 143.886 |
| *IE* (GJ m$^{-2}$) | 57.2410 | 56.7903 |
| *GE* (GJ m$^{-2}$) | 131.3808 | 131.2018 |
| *TE* (GJ m$^{-2}$) | 188.6217 | 187.9921 |
| $S$ (MJ K$^{-1}$ m$^{-2}$) | 205.7494 | 205.7491 |

above. This structure reflects the dominance of the salinity profiles (Fig. 3b) in the density fields. The maximum departure of 4.37 kg m$^{-3}$ is less than half the minimum of $-8.99$ kg m$^{-3}$. The net effect of this density departure on the conservation of mass is to elevate the equilibrium sea surface height 35 cm over that of the ocean. Calculations with a constant-temperature ocean give a similar result, indicating that the change in salinity is responsible for the elevation change. This effect is, in turn, due to the coefficient of saline contraction decreasing with pressure.

Global properties of the ocean and its equilibrium are summarized in Table 3. Mass and salt are conserved between the two systems. Both the internal and gravitational energies are greater for the ocean than its equilibrium, with the internal ($\delta IE = 451$ MJ m$^{-2}$) and gravitational ($\delta GE = 179$ MJ m$^{-2}$) departures contributing 72% and 28%, respectively, to the available energy ($AE = 630$ MJ m$^{-2}$). These departures represent only 0.79% of the total internal energy and 0.14% of the total gravitational energy. Here the gravitational energy is defined to be zero at the 5.5 km depth. The smaller gravitational energy of the equilibrium ocean indicates a lower center of gravity. This lowering occurs despite the slight rise in sea surface elevation and results from the higher stratification (Fig. 3b) of the equilibrium ocean.

The internal energy of the ocean is greater than its equilibrium (Table 3) despite the fact that the equilibrium ocean, with a temperature of 3.66°C, is warmer than the ocean [whose mass-weighted temperature is 3.64°C (Table 2)]. This behavior reflects the nonlinear properties of the internal energy as a function of temperature and pressure. This explanation notes that the rate of change of internal energy with temperature, $\partial u/\partial T$, decreases with pressure. Then the positive temperature anomalies $\delta T > 0$ in the upper ocean produce, on average, a greater positive internal energy change than the negative change produced by the negative departures in the deep ocean (Fig. 3c). The net departure in internal energy is positive, implying an equilibrium ocean with lower internal energy.

The total energy is greater for the ocean than its equilibrium (Table 3). This difference, $\delta TE = 629.5$ MJ m$^{-2}$, agrees within 0.01% with the available energy determined by the minimization of the availability function (Fig. 2). Thus, of the $6.60 \times 10^{25}$ J of total (i.e., internal plus gravitational) energy of the world ocean, only a small fraction, 0.34%, is available to do work and be converted into kinetic energy of macroscopic motions.

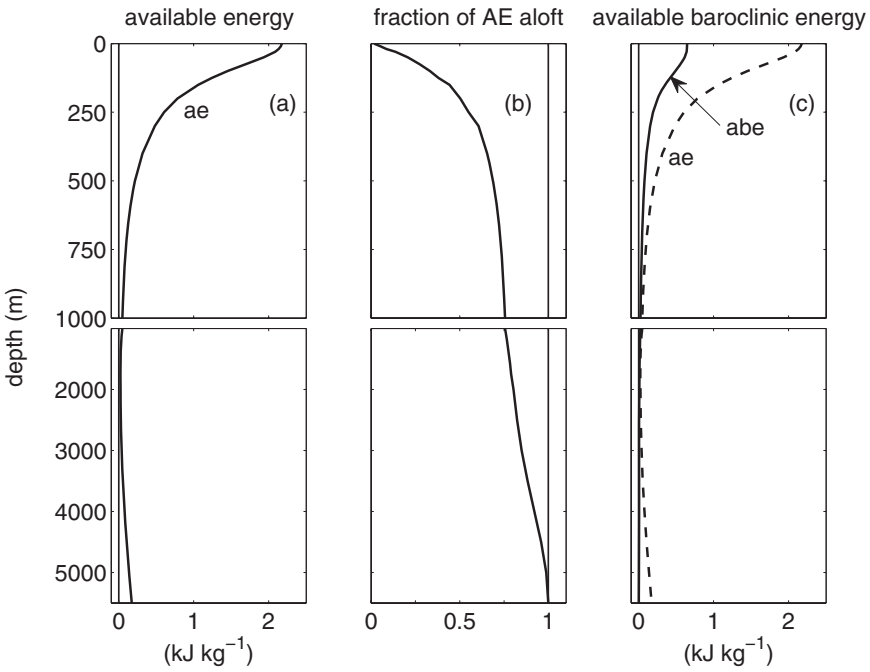


Figure 4. Vertical profiles of (a) the mean specific available energy *ae*, (b) the fraction of total available energy *AE* aloft, and (c) the mean specific available baroclinic energy *abe* (solid curve) and the mean *ae* (dashed curve). The thin vertical lines in each panel represent the reference lines of zero, one, and zero, respectively.

## 3. Ocean energy

### *a. Available energy*

The specific available energy is the availability function (2) evaluated for the equilibrium state

$$ae = \delta h - T_0 \delta s - \alpha \delta p - \mu_0 \delta \chi. \tag{7}$$

The vertical distribution (Fig. 4a) of its horizontal mean indicates a positive-definite field with a maximum value of 2.18 kJ kg$^{-1}$ at the surface and a rapid decline with depth to a minimum of 0.02 kJ kg$^{-1}$ at 1.75 km. Below 2 km there is an increase with depth to a maximum of 0.17 kJ kg$^{-1}$ at a depth of 5.5 km. The definition of the fraction of available energy aloft (Fig. 4b) is

$$f_{AE}(z) = AE^{-1} \int_{A(z)} \int_{z}^{0} \rho \, ae \, dz \, dA_s, \tag{8}$$

where the total available energy $AE$ is $220 \times 10^{21}$ J. The energy is confined mainly to the upper ocean with 50 and 75% above a depth of about 200 and 1,100 m, respectively.

A measure of the baroclinic contribution to the available energy is given by the difference between the available energy and that of the horizontal mean state. We then define the specific available baroclinic energy by

$$abe = ae\,(S_A, T, p) - ae\left(\bar{S}_A, \bar{T}, \bar{p}\right), \tag{9}$$

where the overbar denotes a horizontal area mean. Figure 4c compares this *abe* to the mean available energy. The baroclinic component has a maximum at the surface of 648 J kg$^{-1}$ and deceases with depth. It is significant only above a depth of about 1 km and contributes globally about 29% of the energy. [It is noted that the suggestion of Bannon (2012) to use the lowest equilibrium temperature of a single sounding of the system does not prove to be a useful estimate of the baroclinic contribution for the ocean. The equilibrium temperature is close to the mass-weighted mean temperature of the sounding. For the ocean, that mean sounding is about $-2$°C. Figure 2a indicates that the implied available baroclinic energy is unrealistic.]

Vertical profiles (Fig. 5) of the individual terms in the specific available energy (7) indicate that the enthalpy departure has a slightly larger magnitude than the contribution resulting from the entropy departure (Fig. 5a). The crossing of these two terms with each other and the zero line at a depth of 1.1 km reflects the dominance of the temperature over the salinity field in the enthalpy and entropy departures (Fig. 3a and 3b). The sum of the terms involving enthalpy and entropy overestimates the mean available energy near the surface and yields negative values in the abyss (Fig. 5b). The pressure and concentration departures (Fig. 5c) contribute negatively to the available energy near the surface and positively at great depth. The contribution from the concentration departure closely follows the equilibrium salinity profile, as the variation of the ocean's salinity profile is relatively small (Fig. 3b). The pressure departure contribution to the available energy is small; it is negative above a depth of 4.5 km, reflecting the greater pressure at a given depth of the ocean with respect to its equilibrium state, which is, in turn, due to the greater density of the upper ocean compared to its equilibrium state (Fig. 3c).

Further insight into the structure of the available energy field is afforded by its linearized form (Bannon 2005) that is represented as the sum of the quadratics of the departure of three state variables:

$$ae_{lin} = \frac{T_0}{2c_{p0}}\,(\delta s)^2 + \frac{1}{2\rho_0^2 c_0^2}\,(\delta p)^2 + \frac{\mu_{\chi 0}}{2}\,(\delta \chi)^2, \tag{10}$$

where $c_p$ is the specific heat at constant pressure, $c_0$ is the speed of sound, and $\mu_\chi$ is the derivative of the chemical potential with respect to the concentration. This relation demonstrates that the available energy is positive definite for an ocean close to its equilibrium.

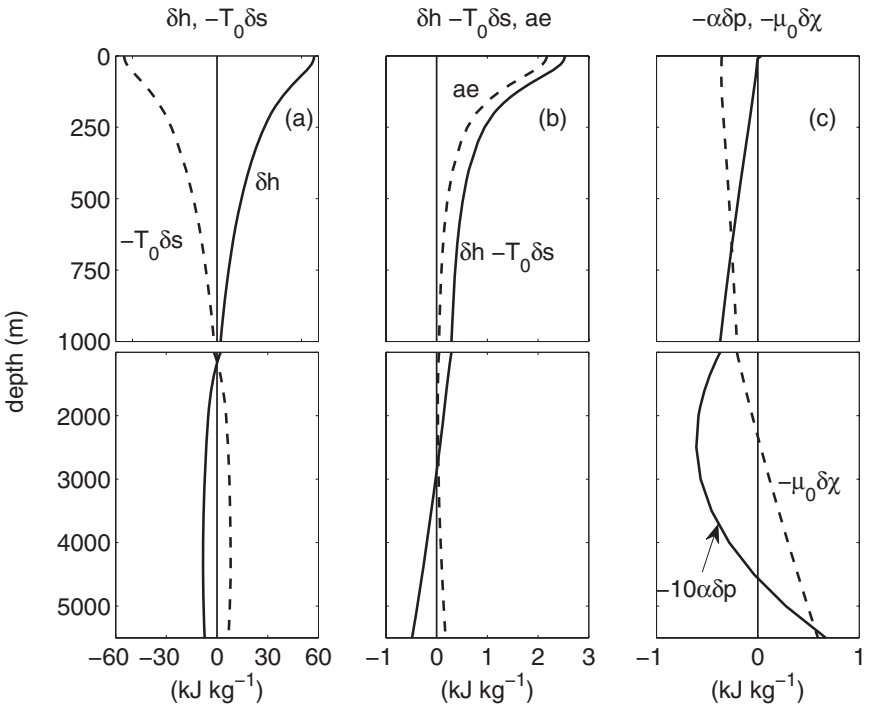


Figure 5. Vertical profiles of (a) the mean departure in the enthalpy (solid curve) and entropy (dashed curve) terms of the available energy, (b) their difference (solid curve) compared to the mean available energy (dashed curve), and (c) the mean departure in pressure multiplied by a factor of 10 (solid curve) and concentration (dashed curve) terms of the specific available energy. The thin vertical line in each panel represents the zero line.

The three terms on the right-hand side of (10) are the linear available potential (*ape*), elastic (*aee*), and chemical (*ace*) energies, respectively. Their mean profiles are plotted in Figure 6. The available potential energy slightly underestimates the mean available energy (Fig. 6a). The mean available elastic energy is negligible with a maximum less than 1 mJ kg$^{-1}$ (not shown). Its coefficient is about $4 \times 10^{-5}$ J kg$^{-1}$ dbar$^{-2}$, implying that a relatively large pressure anomaly of 1 dbar (corresponding to a variation in the sea surface height of 1 m) makes an insignificant contribution. The available chemical energy (Fig. 6b) makes a significant contribution near the surface and in the abyss where the salinity departure is largest (Fig. 3b). The coefficient of the chemical energy contribution represented by the third term is about 2 J kg$^{-1}$ (g kg$^{-1}$)$^{-2}$, implying an energy of 100 J kg$^{-1}$ for a large salinity variation of 10 g kg$^{-1}$. The chemical energy augments the potential one and improves the agreement with the nonlinear result. However, the linear result (10) slightly underestimates the nonlinear one, as shown in Figure 6b where the mean $ae - ae_{linear}$ profile is plotted.

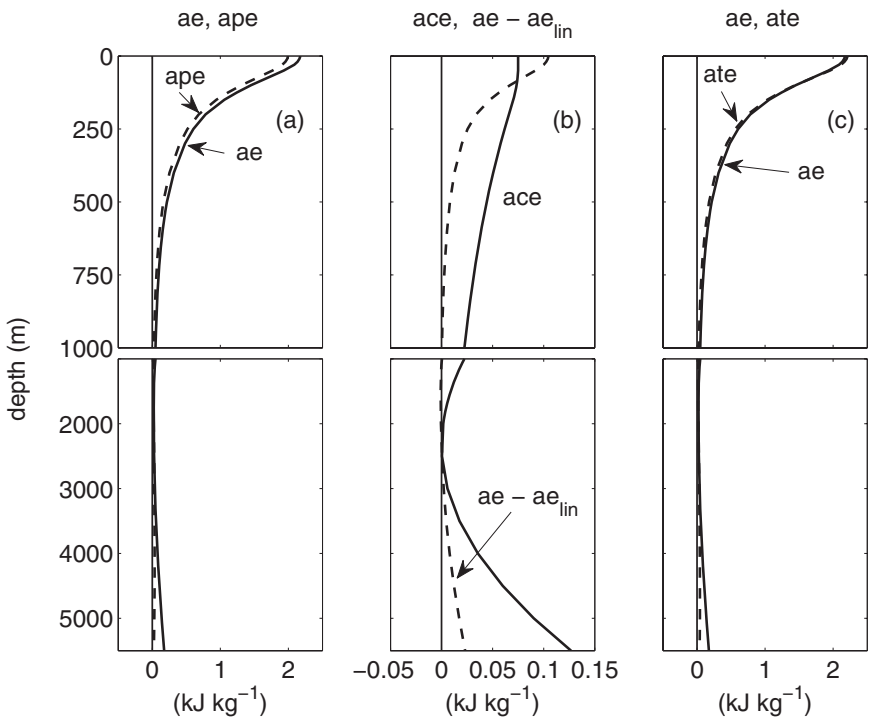


Figure 6. Vertical profiles of (a) the mean available energy (solid curve) and the linear available potential energy (dashed curve), (b) the mean available chemical energy (solid curve) and difference between the mean nonlinear and linear available energies (dashed curve), and (c) the mean available energy (solid curve) and linear available thermal energy (dashed curve). The thin vertical line in each panel represents the zero line.

The preceding analysis of the linear form (10) suggests that the effect of the last two terms in the availability function (2) is small and that the available energy may be approximated by

$$ae \simeq ate \equiv \frac{c_{pt}}{2T_0}\,(\delta T)^2\,, \tag{11}$$

which we designate as the available thermal energy *ate*. We note that this expression is a straightforward approximation of the exergy $\delta h - T_0 \delta s$ for an incompressible liquid. The heat capacity $c_{pt}$ is chosen to produce the best fit to the available energy (7). Table 4 demonstrates the relative accuracy of (11) for four choices of heat capacity: (i) a constant 4.21 kJ kg$^{-1}$ K$^{-1}$ for freshwater at the equilibrium temperature, (ii) a constant 3.99 kJ kg$^{-1}$ K$^{-1}$ for the conservative enthalpy/temperature formulation of McDougall (2003), (iii) for the equilibrium ocean that varies monotonically from an abyssal value of 3.80 kJ kg$^{-1}$ K$^{-1}$ to 4.03 kJ kg$^{-1}$ K$^{-1}$ at the surface, and (iv) for the mean ocean that varies similarly from 3.84

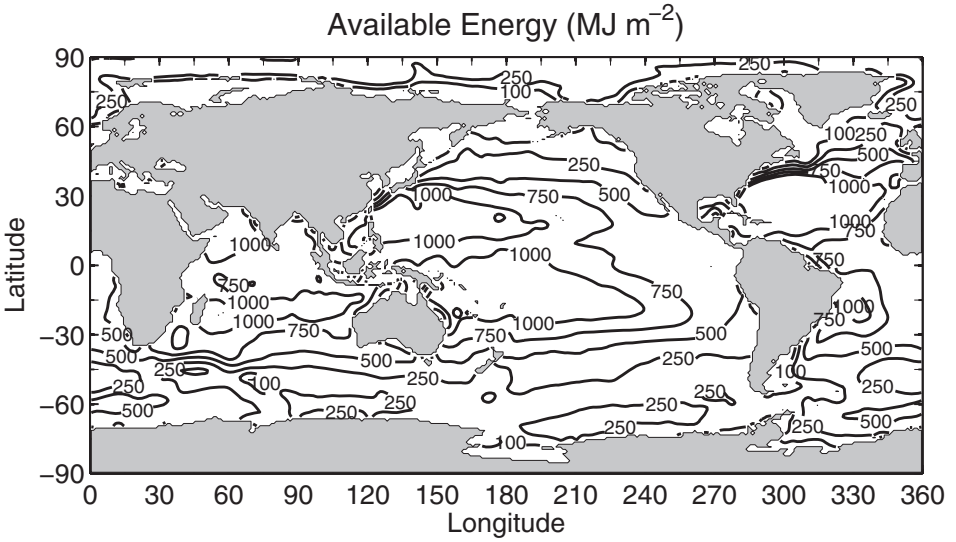


Figure 7. Geographical distribution of the annual mean vertically integrated available energy. The field is smoothed 10 times using a 1–2–1 smoother in both horizontal directions before plotting to eliminate high-frequency noise while retaining the large-scale structure.

Table 4. Accuracy of the available thermal energy *ate* (11) with respect to the exact expression (7) for the specific available energy for various choices of the specific heat $c_{pt}$. The root-mean-square (rms) specific available energy is 1,113 J kg$^{-1}$. The signal-to-noise ratio is the square of the ratio of the standard deviation to the rms error.

| Specific heat | rms error (J kg$^{-1}$) | Signal-to-noise ratio |
|---|---|---|
| Freshwater | 95 | 137 |
| Equilibrium ocean | 56 | 400 |
| Mean ocean | 50 | 496 |
| Conservative temperature | 49 | 519 |

kJ kg$^{-1}$ K$^{-1}$ to 4.00 kJ kg$^{-1}$ K$^{-1}$. The available thermal energy approximation (11) that uses the heat capacity for the conservative temperature most accurately captures the structure of the available energy (Table 4) with a slight underestimate in the thermocline (Fig. 6c). As expected, the abyssal maximum due to salinity is not captured by the approximation (11).

### *b. Geographical distribution of available energy*

The geographical distribution of the vertically integrated available energy (Fig. 7) reflects primarily the temperature distribution (not shown) in the upper ocean. There are subtropical maxima exceeding 1,000 MJ m$^{-2}$ and minima less than 100 MJ m$^{-2}$ in the Bering, Okhotsk,

Table 5. Regional distribution of the departures in internal energy $\delta IE$, gravitational energy $\delta GE$, total energy $\delta TE$, and available energy $AE$ (GJ m$^{-2}$).

| Region | $\delta IE$ | $\delta GE$ | $\delta TE$ | $AE$ |
|---|---|---|---|---|
| Arctic | −25.09 | 0.19 | −24.90 | 0.23 |
| North Atlantic | 27.05 | 0.18 | 27.23 | 0.75 |
| South Atlantic | 2.49 | 0.18 | 2.67 | 0.55 |
| Southern Atlantic | −49.27 | 0.25 | −49.02 | 0.41 |
| Total Atlantic | 3.71 | 0.19 | 3.90 | 0.58 |
| North Pacific | −2.15 | 0.15 | −2.01 | 0.68 |
| South Pacific | 7.24 | 0.17 | 7.41 | 0.70 |
| Southern Pacific | −31.87 | 0.23 | −31.64 | 0.27 |
| Total Pacific | −1.47 | 0.17 | −1.30 | 0.64 |
| Indian | 11.41 | 0.18 | 11.59 | 0.74 |
| Southern Indian | −45.72 | 0.25 | −45.47 | 0.36 |
| Total Indian | 0.54 | 0.19 | 0.73 | 0.67 |
| World ocean | 0.45 | 0.18 | 0.63 | 0.63 |

Chukchi, Greenland, and Argentine Seas. There is a decided zonal asymmetry in the Atlantic and Pacific subtropical basins with larger energies in the west and smaller in the east, reflecting the deeper thermocline in the west. Extreme values of the energy are found in some of the marginal seas as a consequence of the high temperature and salinity in those regions. For example, the Mediterranean Sea has an average available energy of 1,620 MJ m$^{-2}$ for a total of $3.16 \times 10^{21}$ J.

The geographical distributions of the internal, gravitational, and total energies defined by

$$\delta TE = \delta IE + \delta GE, \tag{12}$$

where

$$\delta IE = \int (\rho u - \rho_0 u_0)\, dV \quad \text{and} \quad \delta GE = \int (\rho - \rho_0)\, gz dV. \tag{13}$$

are presented in Table 5. The regional variations associated with the internal energy departure are large and fluctuate in sign. Comparison of Tables 2 and 5 indicates that the fluctuation has the same sign as the mean temperature of the basin minus the equilibrium temperature (3.66°C). In comparison, the gravitational energy fluctuations are all positive in sign and relatively uniform. This uniformity suggests that these fluctuations are primarily due to the relatively consistent difference in the salinity profiles between the ocean and its equilibrium (Fig. 3b). The total energy departures track the departures in internal energy, as the gravitational energy departures are small. We note that the relation (3) stating the equivalence of the available energy and the total energy departure holds globally but not regionally. To emphasize this point, we present the geographical distribution of the available energy in

Table 6. Seasonal variation of available energy (MJ $m^{-2}$) and equilibrium temperature (°C) based on the annual mean and boreal winter, spring, summer, and autumn data sets. The range is the maximum minus the minimum. The maximum for each region is underlined.

| Region | Annual | Winter | Spring | Summer | Autumn | Range |
|---|---|---|---|---|---|---|
| Arctic | 227 | 228 | 228 | 227 | 225 | 3 |
| North Atlantic | 752 | 732 | 739 | 774 | 768 | 42 |
| South Atlantic | 549 | 568 | 559 | 533 | 538 | 35 |
| Southern Atlantic | 411 | 411 | 410 | 412 | 412 | 2 |
| Total Atlantic | 581 | 579 | 579 | 586 | 585 | 7 |
| North Pacific | 676 | 657 | 674 | 694 | 683 | 37 |
| South Pacific | 703 | 721 | 712 | 685 | 697 | 36 |
| Southern Pacific | 265 | 267 | 267 | 262 | 265 | 5 |
| Total Pacific | 641 | 640 | 644 | 641 | 641 | 3 |
| Indian | 744 | 757 | 757 | 731 | 736 | 26 |
| Southern Indian | 357 | 355 | 352 | 361 | 363 | 11 |
| Total Indian | 671 | 680 | 680 | 661 | 665 | 19 |
| World ocean | 630 | 631 | 633 | 629 | 630 | 4 |
| Equilibrium temperature (°C) | 3.655 | 3.657 | 3.660 | 3.653 | 3.652 | 0.008 |

the last column of Table 5. The global departure in total energy is 630 MJ $m^{-2}$, in good agreement with the direct calculation of the available energy (see subsection 2c).

The distribution of total energy departure (Table 5) implies that energy will be exported from regions of positive departure to regions of negative departure during the adjustment to equilibrium. Data from Tables 1 and 5 indicate energy surpluses in the North Atlantic, Indian, South Pacific, and South Atlantic Oceans of 1,190, 686, 565, and 90 ZJ (1 ZJ = $10^{21}$ J) and energy deficits in the Pacific, Indian, and Atlantic regions of the Southern Ocean and the Arctic and North Pacific Oceans of 634, 633, 581, 303, and 159 ZJ, respectively. We note that the implied adjustment process is broadly consistent with a transport of thermal energy from the North Atlantic and subtropical regions to the polar regions.

### *c. Seasonal variation of available energy*

The seasonal variation of the available energy is summarized in Table 6. In these calculations the equilibrium temperature and salinity profiles are determined separately for each data set. The variation in the equilibrium temperature is small. Similarly, the largest variation in the mean equilibrium salinity at any depth is only $7 \times 10^{-4}$ g $kg^{-1}$ (not shown). The North/South Atlantic and Pacific regions exhibit the largest variations of about 5–7% with the maximum occurring in that region's summer. The polar variations are small and can produce maxima in winter (e.g., the Arctic) due to lower temperatures producing a larger variance from the equilibrium temperature. The regional variations tend to compensate to produce a small global variation of less than 1%.

## 4. Discussion

We now discuss how our findings compare with prior estimates of the ocean's available energy. We also consider how neglect of sea ice and variations of sea surface height may affect our available energy estimates.

### *a. Relationship to available potential energy*

The ocean's available energy of 630 MJ $m^{-2}$ is large compared to the available potential energy (APE) estimates of Oort et al. (1989, 1994) and Huang (2005), which lie in the range of 0.4–2.3 MJ $m^{-2}$. Formally we may partition the available energy into two components,

$$AE = \delta TE = TE - TE_0 = APE + TE_a - TE_0, \tag{14}$$

where the subscript $a$ denotes an adiabatic, mechanical rearrangement of individual fluid parcels. Then the Lorenz available potential energy is $APE = TE - TE_a$ and represents a subset of the available energy for an ocean with the same total entropy. (The total entropy of the Lorenz equilibrium state is identical to that of the ocean and to the equilibrium ocean determined here.) The available energy includes a thermodynamic reconfiguration of the system in addition to the Lorenzian, mechanical rearrangement. It therefore subsumes the available potential energy such that $AE \geq APE$.

### *b. Comparison with Bannon (2013)*

The effect of the salinity stratification due to barodiffusion (6) on the available energy is assessed by assuming a uniform salinity as done in Bannon (2013). In that case the mean available energy is reduced about 100 MJ $m^{-2}$ to a value of 523 MJ $m^{-2}$ and the equilibrium temperature decreases slightly to 3.637°C. Thus, about two-thirds of the difference between the present study and that of Bannon (2013) is due to relaxing the assumption of horizontal homogeneity and about one-third is due to a more accurate treatment of salinity in the equilibrium state.

### *c. Sea surface height and sea-ice contributions*

A limitation of these results is the neglect of variations in the ocean's sea surface height $\eta$ and the neglect of sea ice (Fig. 1). Both can in principle be included into the present framework. The gravitational energy departure between the ocean and its equilibrium sea surface height is $(1/2)\rho(z = 0)g\,(\delta\eta)^2$. For a height departure of 1 m, typical of the difference between the sea surface height and the geoid, this energy departure would contribute only $5 \times 10^{-3}$ MJ $m^{-2}$ and may therefore be neglected.

In order to assess the impact of sea ice, we note that the available energy may be partitioned into contributions for each of its components (Bannon 2012; Section 4b) such that $\rho ae = \sum_j \rho_j ae_j$, where the specific available energy of the $j$th component is $ae_j = \delta h_j - T_0 \delta s_j - \alpha_j \delta p_j$. With sea ice residing at the surface, the departures in pressure may, in a

first approximation, be ignored. The enthalpy and entropy of ice (denoted with a subscript $i$) are related to those for the liquid phase (subscript $l$) by the relations $h_i = h_l - l_f$ and $s_i = s_l - l_f/T$, where $l_f$ is the enthalpy of fusion. Then the available energy of the ice is related to that of the liquid by

$$ae_i = ae_l - \left(\frac{T - T_0}{T}\right) l_f\,(T)\,. \tag{15}$$

In order to assess the impact of the sea ice, we take the ice to have a temperature of 0°C ($\delta T = -3.66$ K). Then, using (11) with the conservative temperature value of the specific heat, we find $ae_l \sim 97$ J kg$^{-1}$. In contrast, the phase contribution in (15) is $\leq 4.4 \times 10^3$ J kg$^{-1}$ using the large fusion enthalpy for pure water of $3.34 \times 10^5$ J kg$^{-1}$. A large but representative value of the volume of the sea ice is $5 \times 10^{13}$ m$^3$ (Barry 2011), corresponding to a mass of sea ice of about $5 \times 10^{16}$ kg. Then the available energy of the world sea ice is about $2.2 \times 10^{20}$ J in total or, if distributed uniformly over the Arctic Ocean, 18 MJ m$^{-2}$, corresponding to only an 8% increase in that region (Table 6). Neglecting sea ice in the global available energy analysis is thus a reasonable assumption.

## 5. Available energetics of the ocean

We discuss how available energetics provides a framework for the comparison of thermal and mechanical forcing of the world ocean circulation. The equations describing the available energetics of the ocean are readily obtained (see Appendix) in a manner similar to those for the atmosphere (see Bannon 2012). The ocean's energy balance is governed by the interplay among radiative processes, the mechanical driving by the winds and tidal forces, the efflux of exergy and thermal energy out of the ocean, and the lost work due to irreversible entropy production,

$$\frac{\partial\,(AE + KE)}{\partial t} = \dot{R} - \dot{E} + \dot{W} + \dot{T} - T_0 \dot{S}_{irr}, \tag{16}$$

where $KE$ is the kinetic energy. The available energy generation rate by radiative processes is given by

$$\dot{R} = \int_{V_{ocn}} \left(\frac{T - T_0}{T}\right) \rho \dot{q}_{rad}\, dV, \tag{17}$$

where $\rho\dot{q}_{rad}$ represents the convergence of solar and terrestrial radiation in the upper ocean and $V_{ocn}$ is the volume of the ocean. The rate of generation of kinetic energy by the action of the atmosphere

$$\dot{W} = \int_{A_s} (\mathbf{v} \cdot \tau + \rho_w k e_w \mathbf{v}_w) \cdot \mathbf{n}\, dA, \tag{18}$$

includes that due to the wind stress $\tau$ as well as the kinetic energy input by precipitation, with the subscript $w$ indicating freshwater. Here $\mathbf{n}$ is the unit outward normal to the bounding surface $A_s$ of the ocean. The rate of generation of kinetic energy by tidal action is

$$\dot{T} = -\int_{V_{ocn}} \rho \mathbf{v} \cdot \nabla \Phi_{tidal} dV, \tag{19}$$

where $\Phi_{tidal}$ represents the tidal gravitational potential. The irreversible entropy production is $\dot{S}_{irr} = \int_{V_{ocn}} \dot{s}_{irr} dV$, where $\dot{s}_{irr} \equiv (1/T)\rho\dot{\phi} - (1/T^2)\mathbf{J}_q \cdot \nabla T - \mathbf{J}_s \cdot \nabla(\mu/T) > 0$. This production is positive because the viscous dissipation $\dot{\phi}$ of kinetic energy is always positive, the heat flux $\mathbf{J}_q$ is always down the temperature gradient, and the diffusive flux of salt $\mathbf{J}_s$ is always down the gradient of the relative chemical potential divided by the temperature (de Groot and Mazur 1984). If allowed to operate unopposed, these molecular processes would act to destroy available energy and produce an ocean similar to the equilibrium ocean but with increased entropy. The maximum entropy production occurs when the change in total energy is zero (Landau and Lifshitz 1980). For the world ocean this state has the reference temperature $T_r = 3.694°\text{C}$ (Fig. 2) with a relative chemical potential of 47.45 J g$^{-1}$ salt. The effect of the sensible and latent heat fluxes at the ocean's boundary is given by

$$\dot{E} = \int_{A_s} \left[ \rho_w \, ex_w \, \mathbf{v}_w + \left( \frac{T - T_0}{T} \right) \mathbf{J}_{cond} \right] \cdot \mathbf{n} \, dA, \tag{20}$$

where $ex = \delta h - T_0 \delta s$ is the exergy of freshwater entering or leaving the ocean (by precipitation, evaporation, and fluvial processes) and $\mathbf{J}_{cond}$ is the conductive flux of thermal energy.

The kinetic energy equation is

$$\frac{\partial KE}{\partial t} = \dot{C} + \dot{W} + \dot{T} - \dot{D}, \tag{21}$$

where the conversion of available energy to kinetic energy is

$$\dot{C} = \int_{V_{ocn}} (-\mathbf{v} \cdot \nabla p - \rho \mathbf{v} \cdot \nabla \Phi) dV. \tag{22}$$

This conversion is identical to that of traditional energetics and indicates that seawater flowing down the pressure and geopotential $\Phi$ gradients produces kinetic energy. The rate of dissipation of kinetic energy is $\dot{D} = \int_{V_{ocn}} \rho\dot{\phi} \, dV$ and can feed back into the generation of available energy. In concert with the lost work term, the net generation of available energy by viscous dissipation is $\dot{V} = \int_{V_{ocn}} (T - T_0/T)\rho \, \dot{\phi} \, dV$.

These equations provide an excellent framework (Fig. 8) to compare thermal and mechanical forcings of the ocean's circulation. The equilibrium temperature $T_0$ plays a central role in this comparison through the radiative generation of available energy (17) and the boundary efflux (20). Heating processes are modulated by the efficacy factor $(T - T_0)/T$.

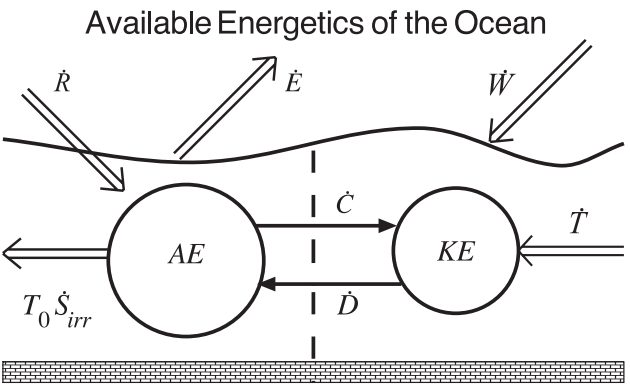


Figure 8. Schematic diagram of the available energetics of the world ocean. Circles denote the reservoirs of available (*AE*) and kinetic (*KE*) energy. Solid arrows indicate the exchange between the reservoirs. Flow down the gradients of pressure and geopotential lead to the conversion $\dot{C}$ of available to kinetic energy. Friction leads to the dissipation $\dot{D}$ of kinetic energy. Open arrows indicate net processes into the total energy reservoir. The ocean is driven by energy inputs by radiation $\dot{R}$, wind stress $\dot{W}$, and tidal forces $\dot{T}$, and by energy outputs of sensible and latent heat $\dot{E}$. The net imbalance is represented by the lost work $T_0\dot{S}_{irr}$ associated with the irreversible production of entropy $\dot{S}_{irr}$. The vertical dashed line conceptually divides the thermodynamic (left) and mechanical (right) domains. For simplicity, benthic processes are omitted.

Although suggestive of the Carnot efficiency, this factor modulates the heating such that a positive heating generates available energy only where the temperature is greater than the equilibrium temperature. For the ocean, where the temperature rarely exceeds 30°C, this efficiency is less than 9% and may become negative. The exergy flux is also dependent on this temperature. The thermal generation of available energy relative to the mechanical generation of kinetic energy by the surface wind stress and tidal forces will be assessed in future work.

## 6. Conclusions

When viewed from an energetics perspective, ocean currents are driven, in part, from the conversion of the ocean's available gravitational and internal energy to kinetic energy. However, the available energy has been difficult to estimate rigorously because the equilibrium state was heretofore unknown. Using a new theory of available energy in geophysical systems (Bannon 2012, 2013), the equilibrium state of the world ocean has been determined by the minimization of an availability function to be a hydrostatic ocean in thermodynamic equilibrium that is isothermal at a temperature of 3.66°C with a salinity profile that is consistent with a uniform relative chemical potential of 47.44 J $g^{-1}$ salt. This equilibrium is in principle accessible by an isentropic reconfiguration of the ocean. The energy difference between the ocean and this equilibrium is available to do work. About 29% of this available

energy is associated with the baroclinic (i.e., horizontal variation) component of the ocean's thermodynamic structure. The remainder lies in the vertical stratification. It has been shown that this available energy is well approximated in terms of the variance of the temperature field relative to the ocean's equilibrium temperature. Thus, the majority of the available energy resides vertically in the upper one-half kilometer of the ocean and geographically mainly in the subtropical gyres.

The value of the oceanic available energy computed here is a small fraction (0.33%) of the total energy in the ocean (Table 3) but, if entirely converted to kinetic energy, would lead to a root-mean-square speed of more than 17 m $s^{-1}$. Some interpretation of this comparison is required. The available energy is the *maximum* amount of work that can be extracted from a system. Processes that extract this work include baroclinic instability, the conversion of the thermal energy associated with the temperature difference across the thermocline to produce electric power, or the conversion of the potential energy of the ocean's salinity profile relative to its equilibrium. However, any geophysically relevant conversion of the available energy is governed by, and hence limited by, the laws of fluid dynamics [see Bannon (2005) for a theoretical discussion of the conversion processes]. Lorenz (1967, 102–103) notes that his "reference state cannot be reached" and that "not all of the APE is 'available'." Similarly, available energy provides a theoretical upper bound on the conversion to kinetic energy. The converse issue is to note that, despite the presence of molecular diffusion of heat and salt, the ocean has been forced externally by the interplay of differential heating, the tides, and the winds into a configuration so far removed from its equilibrium.

*Acknowledgments.* We thank Trevor McDougall and Paul Barker for their assistance with the TEOS-10 Toolbox and reviewer Remi Tailleux and an anonymous reviewer for emphasizing the importance of barodiffusion on the equilibrium salinity gradient. We thank a third reviewer for emphasizing the amplitude of the calculated value of the available energy.

## APPENDIX

### Available energetics of the ocean

This appendix provides a derivation of the governing equations for the oceanic available and kinetic energies. The time rate of change of the available energy (7) following the three-dimensional, mass-weighted, mean velocity **v** is

$$\frac{Dae}{Dt} = \frac{Dh}{Dt} - T_0\frac{Ds}{Dt} - \frac{D}{Dt}(\alpha\delta p) - \mu_0\frac{D\chi}{Dt} - \alpha_0\frac{Dp_0}{Dt}, \tag{A1}$$

where we have used the fact that the equilibrium state satisfies the Gibbs relation in the form $dh = Tds + \alpha dp + \mu d\chi$. Here the material derivative is $D/Dt = \partial/\partial t + \mathbf{v}\cdot\nabla$, $\mathbf{v} = \chi_j\mathbf{v}_j$, and $\chi_j = m_j/\sum_j m_j$, where $m_j$ and $\mathbf{v}_j$ are the mass and velocity of the $j$th component. The subscripts $j = 1$ or 2 (or $j = w$ or $S$) correspond to the freshwater or salt, respectively. The continuity equation is $D\alpha/Dt = \alpha\nabla\cdot\mathbf{v}$, where $\rho = \alpha^{-1}$ is the total density. For

the hydrostatic equilibrium state, the force balance is $\alpha_0 \nabla p_0 = -\nabla\Phi$, where $\Phi$ is the geopotential. Then (A1) becomes

$$\frac{Dae}{Dt} = \frac{Dh}{Dt} - T_0 \frac{Ds}{Dt} - \frac{D}{Dt}(\alpha\delta p) + \mathbf{v} \cdot \nabla\Phi - \mu_0 \frac{D\chi}{Dt}. \tag{A2}$$

The specific kinetic energy, *ke*, and enthalpy, h, equations are

$$\frac{Dke}{Dt} = -\alpha\mathbf{v} \cdot \nabla p - \mathbf{v} \cdot \nabla(\Phi + \Phi_{tidal}) + \alpha\nabla \cdot (\mathbf{v} \cdot \tau) - \dot{\phi}, \tag{A3}$$

$$\frac{Dh}{Dt} = \alpha \frac{Dp}{Dt} + T \frac{Ds}{Dt} + \mu \frac{D\chi}{Dt}, \tag{A4}$$

where $\Phi_{tidal}$ represents the tidal gravitational potential, $\tau$ is the stress tensor, and $\dot{\phi}$ is the viscous dissipation rate. Then (A2), (A3), and (A4) sum to give

$$\frac{D(ae + ke)}{Dt} = -\alpha\nabla \cdot (\delta p\mathbf{v}) + \delta T \frac{Ds}{Dt} + \delta\mu \frac{D\chi}{Dt} + \alpha\mathbf{v} \cdot (\nabla \cdot \tau). \tag{A5}$$

The equation for the salinity rate of change is

$$\rho \frac{D\chi}{Dt} = \rho\dot{\chi} = -\nabla \cdot (\rho_S \mathbf{v}_S), \tag{A6}$$

where $\rho_S$ is the salinity density whose velocity relative to the mass-weighted average velocity $\mathbf{v}$ is $\mathbf{v}'_S = \mathbf{v}_S - \mathbf{v}$. The specific entropy equation is

$$\rho T \frac{Ds}{Dt} = \rho T\dot{s} = \rho\dot{q} + \rho\dot{\phi} - \rho\mu\dot{\chi}, \tag{A7}$$

where $\dot{q}$ is the heating rate due to radiation, conduction, and diffusion. Then (A5) becomes

$$\rho \frac{D(ae + ke)}{Dt} = -\nabla \cdot (\delta p\mathbf{v}) + \nabla \cdot (\mathbf{v} \cdot \tau) + \rho\, sae, \tag{A8}$$

where

$$sae = \left(\frac{\delta T}{T}\right)\dot{q} - \frac{T_0}{T}\dot{\phi} + T_0\left(\frac{\mu}{T} - \frac{\mu_0}{T_0}\right)\dot{\chi}. \tag{A9}$$

It is convenient to rewrite the equation in flux form using the exergy. The exergy of the $j$th component is defined as $ex_j = \delta h_j - T_0\delta s_j$. Then the available energy is $\rho ae = \rho_j ex_j - \delta p$ or $ae = ex - \alpha\delta p$ and the flux form of (A8) is

$$\frac{\partial\rho(ae + ke)}{\partial t} = -\nabla \cdot [\rho(ke + ex)\mathbf{v}] + \nabla \cdot (\mathbf{v} \cdot \tau) - \rho\mathbf{v} \cdot \nabla\Phi_{tidal} + \rho\, sae, \tag{A10}$$

where the rate of working by the pressure departure has dropped from the equation. Decomposing the diabatic term into radiative heating and heat fluxes $\rho\dot{q} = \rho\dot{q}_{rad} - \nabla\cdot\mathbf{J}_q$ yields

$$\frac{\delta T}{T}\rho\dot{q} = \frac{\delta T}{T}\rho\dot{q}_{rad} - \nabla\cdot\left(\frac{\delta T}{T}\mathbf{J}_q\right) + \frac{T_0}{T^2}\mathbf{J}_q\cdot\nabla T. \tag{A11}$$

The third term in (A9) is modified by noting that the $\dot{\chi}$ term may be written in terms of the salt flux relative to the mean flow as $\rho\dot{\chi} = -\nabla\cdot\mathbf{J}_S$, where $\mathbf{J}_S = \rho_S\mathbf{v}'_S = -\mathbf{J}_w$. The last equality follows from mass conservation. Then the third term becomes

$$T_0\left(\frac{\mu}{T} - \frac{\mu_0}{T_0}\right)\rho\dot{\chi} = -T_0\nabla\cdot\left(\frac{\mu}{T} - \frac{\mu_0}{T_0}\right)\mathbf{J}_S + T_0\mathbf{J}_S\cdot\nabla\left(\frac{\mu}{T}\right), \tag{A12}$$

using the fact that $\mu_0/T_0$ is a constant. Collecting these results, we have

$$\rho\, sae = \rho\left(\frac{\delta T}{T}\right)\dot{q}_{rad} - \nabla\cdot\left(\frac{\delta T}{T}\mathbf{J}_q\right) - T_0\nabla\cdot\left(\frac{\mu}{T} - \frac{\mu_0}{T_0}\right)\mathbf{J}_S - T_0\,\dot{s}_{irr}, \tag{A13}$$

where the irreversible entropy production is

$$\dot{s}_{irr} \equiv \frac{1}{T}\rho\dot{\phi} - \frac{1}{T^2}\mathbf{J}_q\cdot\nabla T - \mathbf{J}_S\cdot\nabla\left(\frac{\mu}{T}\right) > 0. \tag{A14}$$

The convergence terms in (A13) can be combined as follows. The heat flux is composed of a conductive flux and a diffusive flux: $\mathbf{J}_q = \mathbf{J}_{cond} + \mathbf{J}_{diff}$, where $\mathbf{J}_{cond} = -k_T\nabla T$ and $\mathbf{J}_{diff} = h_S\mathbf{J}_S + h_w\mathbf{J}_w$. Here $k_T$ is the thermal conductivity of seawater. Then

$$-\nabla\cdot\left(\frac{\delta T}{T}\mathbf{J}_q\right) - T_0\nabla\cdot\left(\frac{\mu}{T} - \frac{\mu_0}{T_0}\right)\mathbf{J}_S = -\nabla\cdot\left(\frac{\delta T}{T}\mathbf{J}_{cond}\right) - \nabla\cdot\mathbf{J}_{ex}, \tag{A15}$$

where the exergy diffusive flux is

$$\mathbf{J}_{ex} = \frac{\delta T}{T}\mathbf{J}_{diff} + T_0\left(\frac{\mu}{T} - \frac{\mu_0}{T_0}\right)\mathbf{J}_S = ex_S\mathbf{J}_S + ex_w\mathbf{J}_w. \tag{A16}$$

The last equality follows with some effort by using the definition of the relative chemical potential.

With these results the available-kinetic energy equation (A10) becomes

$$\begin{aligned}\frac{\partial\rho\,(ae+ke)}{\partial t} = &-\nabla\cdot\left[\rho ke\mathbf{v} + \rho_w ex_w\mathbf{v}_w + \rho_S ex_S\mathbf{v}_S + (\delta T/T)\,\mathbf{J}_{cond}\right]\\ &+\nabla\cdot(\mathbf{v}\cdot\tau) - \rho\mathbf{v}\cdot\nabla\Phi_{tidal} + (\delta T/T)\,\rho\dot{q}_{rad} - T_0\dot{s}_{irr}.\end{aligned} \tag{A17}$$

Integration over the volume of the ocean yields the results discussed in section 5.

REFERENCES

Antonov, J. I., D. Seidov, T. P. Boyer, R. A. Locarnini, A. V. Mishonov, H. E. Garcia, K. Baranova, et al. 2010. World Ocean Atlas 2009, volume 2: Salinity, S. Levitus, ed. NOAA Atlas NESDIS 69. Washington, DC: US Government Printing Office, 184 pp.

Bannon, P. R. 2005. Eulerian available energy in moist atmospheres. J. Atmos. Sci., *62*, 4238–4252.

Bannon, P. R. 2012. Atmospheric available energy. J. Atmos. Sci., *69*, 3745–3762.

Bannon, P. R. 2013. Available energy of geophysical systems. J. Atmos. Sci., *70*, 2650–2654.

Barry, R. G. 2011. The cryosphere—past, present, and future: A review of the frozen water resources of the world. Polar Geogr., *34*, 219–227.

Bejan, A. 2006. Advanced Engineering Thermodynamics, 3rd ed. Hoboken, NJ: Wiley, 880 pp.

Bray, N. A. and N. P. Fofonoff. 1981. Available potential energy for MODE eddies. J. Phys. Oceanogr., *11*, 30–47.

deGroot, S. R. and P. Mazur. 1984. Non-Equilibrium Thermodynamics. New York: Dover, 510 pp.

Feistel, R. 2008. A Gibbs function for seawater thermodynamics for −6 to 80°C and salinity up to 120 g kg$^{-1}$. Deep-Sea Res. I, *55*, 1639–1671.

Fofonoff, N. P. 1962. Physical properties of seawater *in* The Sea, volume 1, M. N. Hill, ed. New York: Wiley-Interscience, 3–30.

Huang, R. X. 2005. Available potential energy in the world's oceans. J. Mar. Res., *63*, 141–158.

Landau, L. D. and E. M. Lifshitz. 1980. Statistical Physics, part I. Oxford: Butterworth-Heinemann, 544 pp.

Landau, L. D. and E. M. Lifshitz. 1987. Fluid Mechanics, 2nd ed. Oxford: Pergamon Press, 539 pp.

Levitus, S. 1982. Climatological Atlas of the World Ocean. NOAA Professional Paper 13. Washington DC: US Government Printing Office, 173 pp.

Locarnini, R. A., A. V. Mishonov, J. I. Antonov, T. P. Boyer, H. E. Garcia, O. K. Baranova, M. M. Zweng, et al. 2010. World Ocean Atlas 2009, volume 1: Temperature, S. Levitus, ed. NOAA Atlas NESDIS 68. Washington, DC: US Government Printing Office, 184 pp.

Lorenz, E. N. 1955. Available potential energy and the maintenance of the general circulation. Tellus, *7*, 157–167.

Lorenz, E. N. 1967. The Nature and Theory of the General Circulation of the Atmosphere. WMO no. 218. Geneva: World Meteorological Organization, 161 pp.

McDougall, T. J. 2003. Potential enthalpy: A conservative oceanic variable for evaluating heat content and heat fluxes. J. Phys. Oceanogr., *33*, 945–963.

McDougall, T. J. and P. M. Barker. 2011. Getting started with TEOS-10 and the Gibbs Seawater (GSW) Oceanographic Toolbox, 28 pp., SCOR/IAPSO WG127, ISBN 978-0-646-55621-5. http://www.teos-10.org/pubs/Getting_Started.pdf

Oort, A. H., L. A. Anderson, and J. P. Peixoto. 1994. Estimates of the energy cycle of the oceans. J. Geophys. Res., *99*, 7665–7688.

Oort, A. H., S. C. Ascher, S. Levitus, and J. P. Peixoto. 1989. New estimates for the available potential energy in the world ocean. J. Geophys. Res., *94*, 3187–3200.

Reid, R. O., B. A. Elliott, and D. B. Olson. 1981. Available potential energy: A clarification. J. Phys. Oceanogr., *11*, 15–29.

Tailleux, R. 2013a. Available potential energy and exergy in stratified fluids. Annu. Rev. Fluid Mech., *45*, 35–58.

Tailleux, R. 2013b. Available potential energy density for a multicomponent Boussinesq fluid with arbitrary nonlinear equation of state. J. Fluid Mech., *735*, 499–518.

Received: *29 July 2013*; revised: *3 September 2014*.